

Detecting entanglement between modes of light

Madhura Ghosh Dastidar¹ and Gniewomir Sarbicki²

¹*Department of Physics, Indian Institute of Technology Madras, Chennai 600036, Tamil Nadu, India*

²*Institute of Physics, Faculty of Physics, Astronomy and Informatics, Nicolaus Copernicus University, Grudziądzka 5/7, 87-100 Toruń, Poland*



(Received 31 January 2022; accepted 2 May 2022; published 30 June 2022)

We consider a subgroup of unitary transformations on a mode of light induced by a Mach-Zehnder Interferometer and an algebra of observables describing a photon-number detector preceded by the interferometer. We explore the uncertainty principles between such observables and their usefulness in performing a Bell-like experiment to show the violation of the Clauser-Horne-Shimony-Holt (CHSH) inequality under the physical assumption that the detector distinguishes between only zero photons and a nonzero number of photons. We show the local settings of the interferometer which lead to a maximal violation of the CHSH inequality.

DOI: [10.1103/PhysRevA.105.062459](https://doi.org/10.1103/PhysRevA.105.062459)

I. INTRODUCTION

Multiphoton entangled states [1,2] have applications in the fields of quantum communication [3], computation [4,5], and metrology [6,7]. In addition to polarization, optical modes of photons are another property that can be entangled, as seen for Dicke superradiant photons [6]. Such quantum states consist of many photons that may be mode entangled.

The Hilbert space of n photons, which can be in two modes (polarization or wave vector), is a symmetric subspace (due to the bosonic nature of photons) of $(\mathbb{C}^2)^{\otimes n}$. If the number of photons in the experiment is not known, then we deal with the direct sum of such spaces having different n 's (Fock space). On the other hand, we can consider a quantum state of light consisting of two modes, each occupied by an arbitrary number of photons. Such a state belongs to the tensor product of the Hilbert spaces of modes, $\mathcal{H}_1 \otimes \mathcal{H}_2$, and may be entangled in general. Further, if we consider two optical modes, the more natural approach is to not have any restrictions on the number of photons. If the number of photons is fixed, then a state of light is supported in an eigenspace of the global photon number, $\hat{N} \otimes \mathbb{I} + \mathbb{I} \otimes \hat{N}$, which is isomorphic to the symmetric sector of $(\mathbb{C}^2)^{\otimes n}$. The whole Hilbert space $\mathcal{H}_1 \otimes \mathcal{H}_2$ is isomorphic to the whole Fock space. In this paper we will consider entanglement of a quantum state of two modes of light, each occupied by an arbitrary number of photons.

In general, entanglement can be detected by estimating the density matrix of the quantum state of the system [8,9] and mathematically testing for its nonseparability using various separability criteria [10]. However, reconstruction of the entire density matrix via quantum state tomography [11] with many photons in each mode is challenging due to the large number of entries in the density matrix, each requiring many measurements to obtain the desired accuracy. Another approach is to measure the expected value of an appropriately chosen entanglement witness [12] and estimate only one parameter instead of all the entries in the density matrix.

The Bell inequality [13,14] is an algebraic expression built from local observables satisfying certain assumptions. The expected value of such an expression satisfies a certain bound for

all separable states. By fixing these observables, one obtains an entanglement witness [15].

The most famous Bell inequality is the Clauser-Horne-Shimony-Holt (CHSH) inequality [16]: $E(A_1 \otimes B_1 + A_1 \otimes B_2 + A_2 \otimes B_1 - A_2 \otimes B_2) \leq 2$. With an appropriate choice of local observables, the CHSH inequality can be violated for certain entangled states with its left-hand side reaching a value of $2\sqrt{2}$, also known as Tsirelson's bound [17].

In Sec. II, we consider the action of a Mach-Zehnder interferometer (MZI) fed with a strong coherent state of light at one input port on a single-mode state of light. We show that, in the limit of a strong coherent field, the MZI setup acts as a unitary operation on the input state, and hence, a projective measurement of the output corresponds to that on its input. However, for finite coherent fields, the action of the MZI setup is rather that of a quantum channel, and the resulting measurement on its input will be a positive operator-valued measure (POVM). In Sec. III, we discuss how in this limit, the quantum channel becomes a unitary transformation and the POVM becomes a projective measurement. We will proceed by considering the limiting scenario in which the MZI realizes a unitary transformation.

Next, in Sec. IV, we discuss the unitary operators related to the action of the MZI and the algebra of the observables representing photon-number measurements preceded by an interferometer. In particular, we discuss uncertainty relations between these observables.

Finally, in Sec. V we discuss how one can perform a Bell-like experiment measuring the violation of the CHSH inequality in such a scenario. We show that, with appropriate setups for the interferometers, we are able to obtain the maximum possible violation of the CHSH inequality.

II. UNITARY TRANSFORMATIONS

For photons, optical components such as beam splitters and phase shifters can be used to generate unitary transformations in the cumulative Fock state.

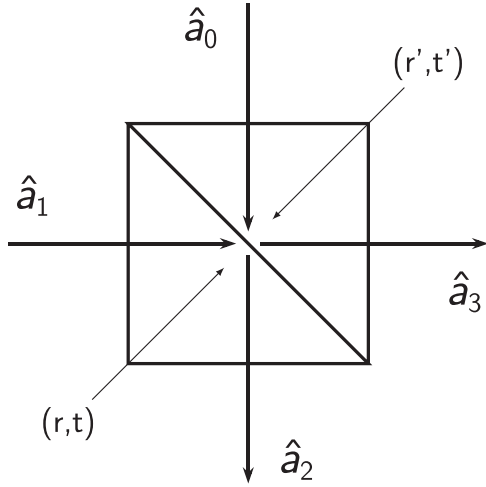


FIG. 1. Quantum beam splitter. Schematic diagram of a quantum beam splitter with two input ports (\hat{a}_0, \hat{a}_1) and two output ports (\hat{a}_2, \hat{a}_3), with corresponding reflectivities and transmittivities at the input (r, t) and output (r', t') ports, respectively.

A. Beam-splitter implementation

The effect of a beam splitter on a photonic state can be envisioned as a unitary operation on the incoming photon states. A typical “quantum” beam-splitter schematic is shown in Fig. 1. The photon-annihilation operators at the output ports (\hat{a}_2, \hat{a}_3) corresponding to the respective input ports (\hat{a}_0, \hat{a}_1) are transformed as [18]

$$\begin{pmatrix} \hat{a}_2 \\ \hat{a}_3 \end{pmatrix} = \begin{pmatrix} t' & r \\ r' & t \end{pmatrix} \begin{pmatrix} \hat{a}_0 \\ \hat{a}_1 \end{pmatrix}, \quad (1)$$

where r and t (r' and t') are the reflectance and transmittance of the beam splitter at the input (output) ports, respectively.

Due to energy conservation, these numbers are complex in general and form a unitary matrix, i.e.,

$$|t|^2 + |r|^2 = 1, \quad (2)$$

$$|t'|^2 + |r'|^2 = 1, \quad (3)$$

$$t'r^* + r't'^* = 0. \quad (4)$$

This implies in particular that $|t| = |t'|$ and $|r| = |r'|$. The above equations are often referred to as Stokes’s laws. In general, for a single photon input, the beam splitter performs a rotation on the Poincaré sphere [19].

Consider a general many-photon Fock state

$$|\psi\rangle = \sum_{n=0}^{\infty} c_n |n\rangle = \sum_{n=0}^{\infty} c_n \frac{1}{\sqrt{n!}} (\hat{a}_0^\dagger)^n |0\rangle \quad (5)$$

and a coherent state of light $\hat{D}_1(\alpha)|0\rangle_1$, where

$$\hat{D}_1(\alpha) = \exp(\alpha \hat{a}_1^\dagger - \alpha^* \hat{a}_1) \quad (6)$$

is the displacement operator, to be incident on the first and second ports of the beam splitter (BS), respectively. The total input state of the BS is

$$|\psi\rangle_0 \otimes |\alpha\rangle_1 = \sum_{n=0}^{\infty} c_n \frac{1}{\sqrt{n!}} (\hat{a}_0^\dagger)^n |0\rangle_0 \otimes \hat{D}_1(\alpha) |0\rangle_1. \quad (7)$$

Assuming the beam splitter operator is \hat{U}_1 , from (1), we get the photon-annihilation operators (\hat{a}_0 and \hat{a}_1) in terms of those at the output ports (\hat{a}_2 and \hat{a}_3) as

$$\hat{a}_0 = t'^* \hat{a}_2 + r'^* \hat{a}_3, \quad \hat{a}_1 = r^* \hat{a}_2 + t^* \hat{a}_3, \quad (8)$$

where we have used Stokes’s laws, $r^*t' + r't^* = 0$ and $|r|^2 + |t|^2 = 1$, along with Eq. (1).

Applying the BS transformation (1) to operators in the input-state formula (7), we obtain

$$\begin{aligned} & |\psi\rangle_0 \otimes |\alpha\rangle_1 \xrightarrow{\text{BS}} |\Psi\rangle_{\text{out}} \\ &= \exp[\alpha(r\hat{a}_2^\dagger + t\hat{a}_3^\dagger) - \alpha^*(r^*\hat{a}_2 + t^*\hat{a}_3)] \sum_{n=0}^{\infty} \frac{c_n}{\sqrt{n!}} (t'\hat{a}_2^\dagger + r'\hat{a}_3^\dagger)^n |0\rangle_2 \otimes |0\rangle_3 \\ &= \exp(r\alpha\hat{a}_2^\dagger - r^*\alpha^*\hat{a}_2) \exp(t\alpha\hat{a}_3^\dagger - t^*\alpha^*\hat{a}_3) \sum_{n=0}^{\infty} c_n \frac{1}{\sqrt{n!}} (t'\hat{a}_2^\dagger + r'\hat{a}_3^\dagger)^n |0\rangle_2 \otimes |0\rangle_3 \\ &= \hat{D}_2(r\alpha) \hat{D}_3(t\alpha) \sum_{n=0}^{\infty} c_n \frac{1}{\sqrt{n!}} (A^\dagger)^n |0\rangle_2 \otimes |0\rangle_3, \end{aligned} \quad (9)$$

where $A^\dagger = t'\hat{a}_2^\dagger + r'\hat{a}_3^\dagger$. In the limit of a highly reflective beam splitter and a highly intense coherent state,

$$r \rightarrow 1, \quad t\alpha = \text{const}, \quad (10)$$

the output-state formula (9) reduces to

$$|\Psi\rangle_{\text{out}} = |r\alpha\rangle_2 \otimes \hat{D}_3(t\alpha)|\psi\rangle_3. \quad (11)$$

Thus, we achieve the incoming coherent state with reduced intensity $|r\alpha\rangle_2$ and the incoming photonic state displaced by $t\alpha$ at output ports 2 and 3, respectively. The separability of the

state (11), i.e., of the two output modes, is desired, and we obtain a unitary transformation of the incoming photonic state. A realistic (finite α) description involves more summands in (11). Tracing out output 2, we will obtain a quantum channel between input 0 and output 3. By terminating output 3 with a photodetector, we obtain a POVM on the input photonic state. We will discuss this situation in detail in Sec. III.

Using the above result in which the beam splitter displaces any quantum state, we can physically implement unitary transformations over the photonic wave packet. However, in this case, the parameters of displacement, i.e., t and α , depend

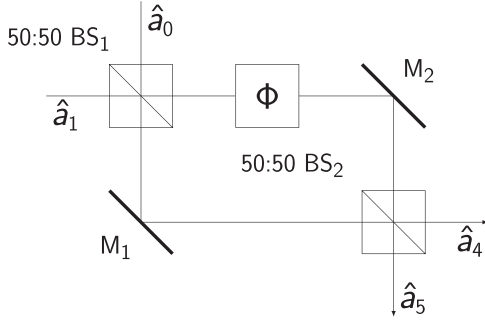


FIG. 2. Mach-Zehnder interferometer. MZI setup with a phase shift ϕ in one of the arms of the interferometer. Two 50:50 beam splitters (BS_1 and BS_2 , with BS_2 rotated 180° with respect to BS_1) with equal magnitudes of reflectivity and transmittivity are used along with two mirrors (M_1 and M_2) for such an interferometer.

only on the transmittivity of the beam splitter and the input coherent field intensity, respectively. Moreover, a highly reflective beam splitter with $r \rightarrow 1$ is practically difficult to construct. To eliminate such problems with the implementation of the scheme and to exercise a further degree of tunability of the displacement operator, we describe the case of using a MZI setup with the same input state [see Eq. (7)].

B. Mach-Zehnder interferometric implementation

A MZI can be approximated as a four-port device [20] as shown in Fig. 2. The composite optical elements of the MZI setup each correspond to a unitary operation over the field states. We define the matrix associated with the effect of the phase shifter over the input state as

$$P_\phi = \begin{pmatrix} 1 & 0 \\ 0 & e^{i\phi} \end{pmatrix}. \quad (12)$$

Using the definition of the beam-splitter operator from Eq. (1), we find the transformation of the annihilation operators to be

$$\begin{pmatrix} \hat{a}_4 \\ \hat{a}_5 \end{pmatrix} = \begin{pmatrix} t'_2 & r_2 \\ r'_2 & t_2 \end{pmatrix} \begin{pmatrix} 1 & 0 \\ 0 & e^{i\phi} \end{pmatrix} \begin{pmatrix} t'_1 & r_1 \\ r'_1 & t_1 \end{pmatrix} \begin{pmatrix} \hat{a}_0 \\ \hat{a}_1 \end{pmatrix}.$$

Now, assuming that two identical beam splitters are arranged in the MZI setting such that the first beam splitter is aligned in the reverse direction relative to the second as shown in Fig. 2, we have

$$\begin{aligned} \begin{pmatrix} \hat{a}_4 \\ \hat{a}_5 \end{pmatrix} &= \begin{pmatrix} t' & r \\ r' & t \end{pmatrix} \begin{pmatrix} 1 & 0 \\ 0 & e^{i\phi} \end{pmatrix} \begin{pmatrix} t'^* & r'^* \\ r'^* & t^* \end{pmatrix} \begin{pmatrix} \hat{a}_0 \\ \hat{a}_1 \end{pmatrix} \\ &= \begin{pmatrix} |t'|^2 + |r|^2 e^{i\phi} & r'^* t' (1 - e^{i\phi}) \\ r' t'^* (1 - e^{i\phi}) & |r'|^2 + |t|^2 e^{i\phi} \end{pmatrix} \begin{pmatrix} \hat{a}_0 \\ \hat{a}_1 \end{pmatrix}, \end{aligned}$$

using Eq. (4). Now, we assume both are 50:50 beam splitters, i.e., $|t| = |t'| = |r| = |r'| = \frac{1}{\sqrt{2}}$. Also since all coefficients of reflection and transmission are complex numbers, we can write $r' = |r'| e^{i\gamma_1}$ and $t' = |t'| e^{i\gamma_2}$. Therefore, the above equation reduces to

$$\begin{pmatrix} \hat{a}_4 \\ \hat{a}_5 \end{pmatrix} = \frac{1}{2} \begin{pmatrix} 1 + e^{i\phi} & e^{i\gamma} (1 - e^{i\phi}) \\ e^{-i\gamma} (1 - e^{i\phi}) & 1 + e^{i\phi} \end{pmatrix} \begin{pmatrix} \hat{a}_0 \\ \hat{a}_1 \end{pmatrix}, \quad (13)$$

where $\gamma = \gamma_2 - \gamma_1$. Alternating the roles of \hat{a}_4 and \hat{a}_5 , we get

$$\begin{pmatrix} \hat{a}_5 \\ \hat{a}_4 \end{pmatrix} = \begin{pmatrix} T' & R \\ R' & T \end{pmatrix} \begin{pmatrix} \hat{a}_0 \\ \hat{a}_1 \end{pmatrix}, \quad (14)$$

where

$$\begin{aligned} R &= R' = \frac{1 + e^{i\phi}}{2}, & T &= \frac{e^{i\gamma} (1 - e^{i\phi})}{2}, \\ T' &= \frac{e^{-i\gamma} (1 - e^{i\phi})}{2}. \end{aligned} \quad (15)$$

Thus, the MZI scattering matrix is equivalent to that of a beam splitter with tunable parameters, namely, effective reflectivities (R and R') and transmittivities (T and T').

In the limit $\phi \rightarrow 0$, we can use the Taylor expansion of $e^{i\phi}$ up to the second term such that $1 - e^{i\phi} \simeq -i\phi$. So Eqs. (15) are modified to

$$\lim_{\phi \rightarrow 0} R = \lim_{\phi \rightarrow 0} \frac{2 + i\phi}{2} \simeq 1, \quad (16)$$

$$\lim_{\phi \rightarrow 0} T = \lim_{\phi \rightarrow 0} -\frac{i\phi}{2} e^{i\gamma} \simeq 0. \quad (17)$$

Drawing an analogy to Sec. II A, we would require $T\alpha$ to remain constant [see Eq. (10)]. For this, $|\alpha| \sim 1/\phi$. The proportionality constant and phase of α will establish a proper displacement in Eq. (11). We are able to displace the input quantum state by $T\alpha$ using a MZI setup with two identical 50:50 beam splitters and small phase difference between the arms, fed by a strong laser field in a coherent state.

In the case when α is finite, the state of the outputs is weakly entangled and tends to a separable state when $\alpha \rightarrow \infty$. This leads to a quantum channel realized by the MZI instead of a unitary transformation. Terminating the output with a detector will result in a POVM on the input state. We will explain this approach in the next section.

III. POVMs

Let us assume from now on that the bottom arm of the MZI setup is ended by a photon-number detector; that is, we measure the intensity of the field represented by the photon-number operator $\hat{N} = \hat{a}^\dagger \hat{a}$. The MZI setup applies a global unitary transformation on the product state of the composite system (coherent state + multiphoton state). Let the projectors on the coherent and multiphoton states be $\sigma = |\alpha\rangle\langle\alpha|$ and $\rho = |\psi\rangle\langle\psi|$, respectively.

Thus, the state of the outputs of the MZI setup fed by an input state $\sigma \otimes \rho$ is

$$\varepsilon = U(\sigma \otimes \rho)U^\dagger, \quad (18)$$

where U is the unitary operation performed by the MZI setup. Note that U has infinite dimensionality in the Schrödinger picture. The blocks of the matrix ε are

$$\varepsilon_{mn} = \text{Tr}_1(\varepsilon |m\rangle\langle n| \otimes \mathbb{I}) = \sum_{ij} U_{mi}(\sigma_{ij\rho})(U_{nj})^\dagger, \quad (19)$$

where U_{mi} is the m th block of U .

In the standard Fock basis, $\sigma_{ij} = \langle i|\alpha\rangle\langle\alpha|j\rangle \equiv \alpha_i \alpha_j^*$. Substituting σ_{ij} in Eq. (19) and evaluating the trace of this quantum operation with respect to the first subsystem σ , we

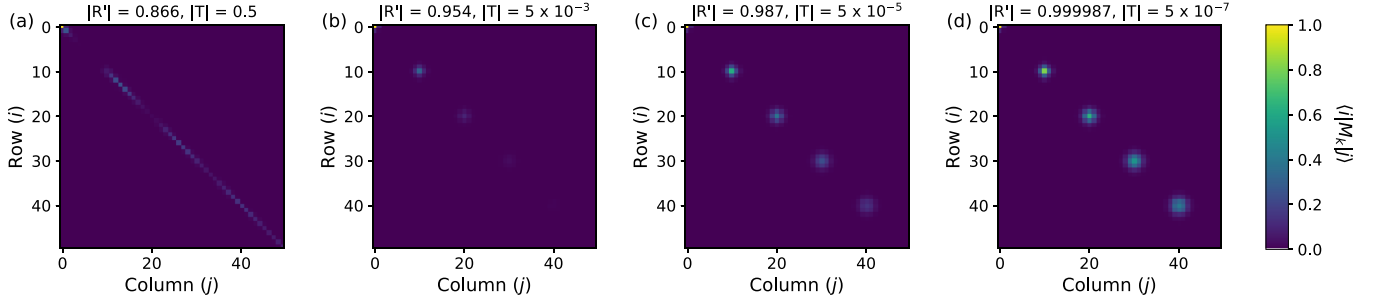


FIG. 3. POVM element M_k : Numerically generated plot of the absolute values of matrix elements of operators M_k , restricted to their top left block with a size of 50×50 . Each graph shows data for $k \in \{0, 10, \dots, 40\}$. $T\alpha = 0.1$ is kept constant, and the graphs show the data for (a) $|R'| = 0.866$, $|T| = 0.5$; (b) $|R'| = 0.954$, $|T| = 5 \times 10^{-3}$; (c) $|R'| = 0.987$, $|T| = 5 \times 10^{-5}$; and (d) $|R'| = 0.999987$, $|T| = 5 \times 10^{-7}$. The color bar (on the right) indicates the absolute values of the respective matrix entries. The axes of each graph are the column and row indices of the matrix.

obtain

$$\varepsilon = \sum_k \sum_{ij} (\alpha_i U_{ki}) \rho (\alpha_j U_{kj})^\dagger = \sum_k E_k \rho E_k^\dagger, \quad (20)$$

where $E_k = \sum_i \alpha_i U_{ki}$ act as Kraus operators. It can easily be checked that these operators satisfy the completeness relation $\sum_k E_k E_k^\dagger = \mathbb{I}$ (trace preservation).

The probability of observing i photons at the detector is

$$\begin{aligned} p(i) &= \text{Tr} \left[|i\rangle\langle i| \sum_k \left(\sum_j \alpha_j U_{kj} \right) \rho \left(\sum_j \alpha_j U_{kj} \right)^\dagger \right] \\ &\equiv \text{Tr}(M_i \rho), \end{aligned} \quad (21)$$

where $M_i = \sum_k (\alpha_j U_{kj})^\dagger |i\rangle\langle i| (\alpha_j U_{kj})$ is the effect corresponding to measuring i photons at the output. Using Eq. (9), we derive this effect for the MZI setting:

$$\begin{aligned} M_i &= e^{-|T\alpha|^2} \frac{|T\alpha|^{2i}}{i!} \sum_{n, n'=0}^{\infty} (-R'^* T\alpha)^{n'} (-R'^* T\alpha)^{*n} \\ &\times \sum_{k=0}^{\min\{n, n'\}} \frac{|R'\alpha|^{-2k}}{k!} \frac{\sqrt{n'!n!}}{(n'-k)!(n-k)!} \\ &\times \sum_{j=0}^{\min\{i, n'-k\}} \frac{i!(n'-k)!(-|T\alpha|)^{-2j}}{j!(i-j)!(n'-k-j)!} \\ &\times \sum_{j=0}^{\min\{i, n-k\}} \frac{i!(n-k)!(-|T\alpha|)^{-2j}}{j!(i-j)!(n-k-j)!} |n'\rangle\langle n|. \end{aligned} \quad (22)$$

In the limit $|R'| \rightarrow 1$, $T\alpha = \text{const}$ (discussed in Sec. II B), only the summand corresponding to $k=0$ survives in Eq. (22), and M_i reduces to a projector onto the state vector $|i, T\alpha\rangle = \hat{D}(T\alpha)|i\rangle$ of a generalized coherent state (GCS):

$$M_i \rightarrow \hat{D}^\dagger(T\alpha)|i\rangle\langle i|\hat{D}(T\alpha), \quad (23)$$

and we obtain a projective measurement as the limiting case. (See Appendix A for details.)

In Fig. 3 we show the numerically obtained matrix representations of M_i ($i \in \{0, 10, \dots, 40\}$) for different values of $|R'|$ and $|T|$ in the MZI setup. From Figs. 3(a) to 3(d), the values of R' and T slowly approach the limit of $|R'| = |R| \rightarrow 1$,

$T \rightarrow 0$, and $\alpha \rightarrow \infty$ under the condition that $T\alpha$ remains constant.

Next, we numerically estimate the overlap $\langle M_j | M_i \rangle_{HS} = \text{Tr}(M_j^\dagger M_i)$ between the effects of M_i and M_j for each $i, j \in [0, 40]$, estimating the effects' operators using 52×52 matrices. We arrange the overlaps into a square matrix, which is the (top left block of a) Gram matrix of the POVMs. We plot the absolute values of its entries in the logarithmic scale [see Figs. 4(a)–4(d)]. We observe that for $|R'| = 0.999987$ and $|T| = 5 \times 10^{-7}$, we obtain an almost diagonal matrix, as expected for almost orthonormal operators M_i approximating the projective measurement.

IV. MAASSEN-UFFINK UNCERTAINTY PRINCIPLE

In the previous section, we described the POVMs associated with the measurement made by a photon-number detector in one arm of the MZI setting. While the MZI setup realizes the displacement operator $\hat{D}(\beta)$ under certain limits (discussed in Secs. II B and III), the setup MZI + detector measures the observable $\hat{D}^\dagger(\beta)\hat{N}\hat{D}(\beta)$. We would like to comment now on the uncertainty relation between two such observables for two different values of β .

The Maassen-Uffink uncertainty principle [21] deals with entropic uncertainties relying on Shannon entropy as a measure of uncertainty. The probability distributions for any quantum state $|\psi\rangle$ with respect to two observables A and B having sets of eigenvectors $|a_j\rangle$ and $|b_j\rangle$ are $p = |\langle a_j | \psi \rangle|^2$ and $q = |\langle b_j | \psi \rangle|^2$, respectively. The Shannon entropy corresponding to any general probability distribution $x = (x_1, \dots, x_N)$ is given as $H(x) = -\sum_j x_j \log_2 x_j$. For an N -dimensional Hilbert space, the Maassen-Uffink uncertainty principle is given as

$$H(p) + H(q) \geq -2 \log_2 c, \quad (24)$$

where $c = \max_{j,k} |\langle a_j | b_k \rangle|$. The right-hand side of Eq. (24) is independent of $|\psi\rangle$, i.e., the state of the system. Thus, nontrivial information is gathered about the probability distributions p and q from this relation, provided $c < 1$.

In the context of our problem, first, we need to estimate the lower bound in Eq. (24). The observables $\hat{D}^\dagger(\beta_1)\hat{N}\hat{D}(\beta_1)$, $i \in \{1, 2\}$, have eigenbases $\{D^\dagger(\beta_i)|n\rangle\}$. We want to find the maximum of $|\langle m | D(\beta_1) D^\dagger(\beta_2) | n \rangle| = |\langle m | D(\beta_1 - \beta_2) | n \rangle|$

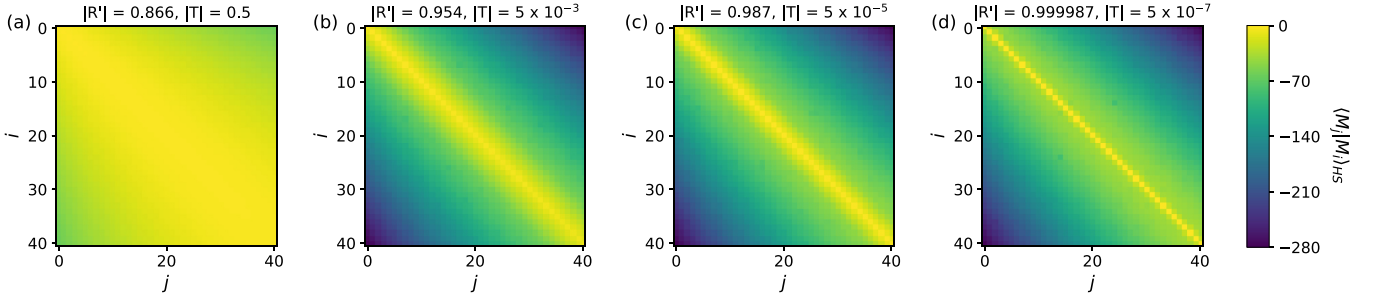


FIG. 4. Overlap between M_i and M_j : Numerically generated plot (in logarithmic scale) for the overlap $\text{Tr}(M_i M_j)$ between POVMs, where $i, j \in \{0, \dots, 39\}$. $T\alpha$ is kept constant, and the graphs show the data for (a) $|R'| = 0.866$, $|T| = 0.5$; (b) $|R'| = 0.954$, $|T| = 5 \times 10^{-3}$; (c) $|R'| = 0.987$, $|T| = 5 \times 10^{-5}$; and (d) $|R'| = 0.999987$, $|T| = 5 \times 10^{-7}$. The color bar (on the right) indicates the natural logarithm of the absolute value of the overlap. The axes denote the labels (i, j) of POVM effects M_i and M_j , i.e., the effects corresponding to detection of the i th and j th photons at the detector.

over n, m . Let us provide the notation $\beta = \beta_1 - \beta_2$. The displacement operator $\hat{D}(\beta)$ acting on a state vector $|n\rangle$ produces a GCS [22–24], which can be decomposed in the occupancy-number basis as

$$|n, \beta\rangle = \hat{D}(\beta)|n\rangle = \sum_{k=0}^{\infty} C_{n,k}|k\rangle,$$

where

$$C_{n,k} = e^{-|\beta|^2/2} \sum_{i=0}^{\min(n,k)} \frac{\sqrt{n!}(-\beta^*)^{n-i}}{\sqrt{i!(n-i)!}} \frac{\sqrt{k!}(\beta)^{k-i}}{\sqrt{i!(k-i)!}} \quad (25)$$

(see Appendix B).

Now, numerically analyzing $C_{n,k}$ [Eq. (25)] for many values of β , we have obtained the following observation:

Conjecture 1. The maximum of $|C_{n,k}|$ is realized for $n = 0$ (or $k = 0$) (see Fig. 5).

Using the above conjecture, we proceed analytically. It is straightforward to observe that the sequence $C_{0,k}$ (the coefficients of a coherent state in the occupancy-number basis) satisfies the recurrence relation $C_{0,k} = \frac{\beta}{\sqrt{k}} C_{0,k-1}$, and we easily observe that $\max_k |C_{0,k}|$ is at $k = |\beta|^2$ (rounded to one of the nearest integers). Hence, we get

$$\max_{n,k} |C_{n,k}| = |C_{0,|\beta|^2}| = e^{-|\beta|^2/2} \frac{|\beta|^{|\beta|^2}}{\sqrt{\Gamma(|\beta|^2 + 1)}}. \quad (26)$$

Applying Stirling's formula to $\Gamma(|\beta|^2 + 1)$, i.e., $\Gamma(|\beta|^2 + 1) > \sqrt{2\pi|\beta|^2} \left(\frac{|\beta|^2}{e}\right)^{|\beta|^2}$, we have

$$|C_{0,|\beta|^2}| < e^{-|\beta|^2/2} \frac{|\beta|^{|\beta|^2}}{[\sqrt{2\pi|\beta|^2} \left(\frac{|\beta|^2}{e}\right)^{|\beta|^2}]^{1/2}}. \quad (27)$$

On simplifying the above equation, we arrive at

$$|C_{0,|\beta|^2}| < \frac{1}{\sqrt[4]{2\pi|\beta|^2}}; \quad (28)$$

hence, $c < (2\pi|\beta|^2)^{-1/4}$, and Eq. (24) gives us

$$H(p) + H(q) \geq \frac{1}{2} \log_2(2\pi|\beta_1 - \beta_2|^2), \quad (29)$$

where $p_i = |\langle i|\hat{D}(\beta_1)|\psi\rangle|^2$, $q_i = |\langle i|\hat{D}(\beta_2)|\psi\rangle|^2$, and $|\beta| = |\beta_1 - \beta_2|$. In a finite-dimensional Hilbert space, the bound in

Eq. (24) is for a pair of observables with unbiased eigenbases (related by a Hadamard unitary matrix) and cannot exceed $\log_2 d$, where d is the dimension of the Hilbert space. In our case, the dimension of the Hilbert space is infinite, and the bound in Eq. (29) is unbounded and grows with the modulus of the difference between the displacements β_1 and β_2 .

V. CHSH INEQUALITY

In this section, we consider a situation in which two modes of light in an entangled state are separated and sent to two distant laboratories, each possessing a MZI. If both sides independently choose one of the two settings of displacements (described below) of their MZIs in subsequent measurements, one can verify whether the celebrated CHSH inequality is violated by the measurement data. The violation of the CHSH

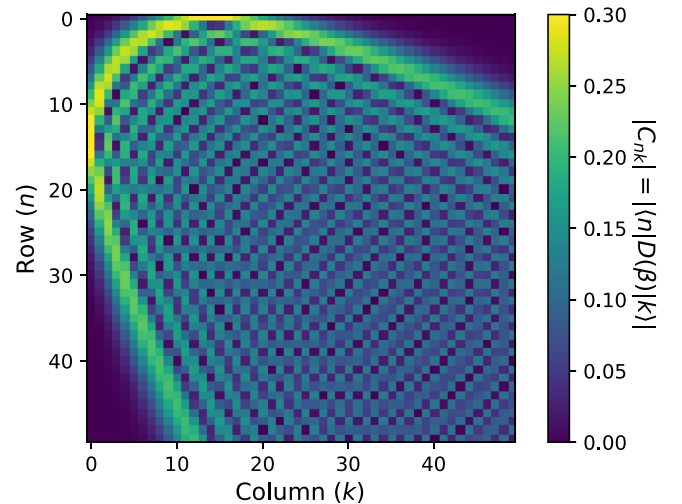


FIG. 5. Displacement operator: matrix elements. Numerically generated plot for the absolute value of the matrix element ($|C_{n,k}| = |\langle n|\hat{D}(\beta)|k\rangle|$, with $n, k \in \{0, \dots, 49\}$) of the displacement operator $\hat{D}(\beta)$ for $\beta = 3.8$. $|n\rangle$ and $|k\rangle$ are elements of the eigenbasis of the photon-number operator. The x and y axes represent k and n , respectively, and hence the column and row indices of the matrix element. The color bar (on the right) indicates the absolute values of the plotted matrix entries.

inequality is seen as the experimental confirmation of the entangled nature of the concerned states [16]. Therefore, in this section we consider the local MZI settings that lead to the best test for the entanglement and look for a multiphoton two-mode state $|\psi\rangle$ for which entanglement is best indicated.

A. CHSH inequality for infinite intensities of coherent states

Recently, a scheme for photon-number-resolved detection of a multiphotonic wave packet was proposed [25] and implemented in experiment. As we require dichotomic observables for modeling the CHSH inequality for our problem, we consider a photodetector that gives binary measurement outcomes. Therefore, when the detector is placed at the output port of the MZI setting, either zero photons or a nonzero number of photons will be reported by the detector. Let us prescribe the outputs -1 and 1 to these possibilities. The related observable will be

$$A(\beta) = (-1)|\beta\rangle\langle\beta| + (+1)(\mathbb{I} - |\beta\rangle\langle\beta|) = \mathbb{I} - 2|\beta\rangle\langle\beta|. \tag{30}$$

Here $|\beta\rangle = \hat{D}^\dagger(\beta)|0\rangle$ is the vector corresponding to the measurement output of -1 .

Let us assume that we have two such observables $A(\beta_1)$ and $A(\beta_2)$. For a state vector Ψ , the output statistics of both observables will be determined by the two probabilities of getting an output of -1 for each of them:

$$p(A_i = -1|\Psi) = |\langle\Psi|\beta_i\rangle|^2, \quad i = 1, 2. \tag{31}$$

The output statistics is determined by the projection of Ψ ($\Pi_V\Psi$) onto $V = \text{span}\{\beta_1, \beta_2\}$. While $\Pi_V\Psi$ can have an arbitrary norm ≤ 1 , the effective Hilbert space must have at least one direction orthogonal to V to project a normalized Ψ onto $\Pi_V\Psi$ of the desired norm. One orthogonal direction is enough to obtain it, and hence, the dimension of the effective Hilbert space for both observables is 3.

Let us fix an orthonormal basis of the effective Hilbert space \mathcal{H} . Assuming that the displacement applied is $-\beta_1$ or $-\beta_2$, let

$$\begin{aligned} |e_1\rangle &= |\beta_1\rangle, \\ |e_2\rangle &= \frac{|\beta_2\rangle - \langle\beta_1|\beta_2\rangle|\beta_1\rangle}{\sqrt{1 - |\langle\beta_1|\beta_2\rangle|^2}} \\ &= \frac{|\beta_2\rangle - \langle\beta_1|\beta_2\rangle|\beta_1\rangle}{\sqrt{1 - \exp(-|\beta_1 - \beta_2|^2)}}, \end{aligned} \tag{32}$$

and let $|e_3\rangle$ be an arbitrary vector orthogonal to $|\beta_1\rangle, |\beta_2\rangle$. Considering $\{|e_1\rangle, |e_2\rangle, |e_3\rangle\}$ as the basis for \mathcal{H} , the observables A_1 and A_2 are represented by matrices:

$$A(\beta_1) = \begin{pmatrix} -1 & 0 & 0 \\ 0 & 1 & 0 \\ 0 & 0 & 1 \end{pmatrix}, \tag{33}$$

$$A(\beta_2) = \begin{pmatrix} 1 - 2E & -2\sqrt{E(1-E)} & 0 \\ -2\sqrt{E(1-E)} & -1 + 2E & 0 \\ 0 & 0 & 1 \end{pmatrix}, \tag{34}$$

where $E = \exp(-|\beta_1 - \beta_2|^2)$.

Let us assume that we have a source producing copies of a two-mode, multiphoton state. Consider an experiment in which these two modes become spatially separated and for each state from the pair simultaneous measurements are performed in two distant laboratories. The first laboratory chooses the displacement in the MZI setup to be $-\beta_1$ or $-\beta_2$ randomly, measuring the observables $A(\beta_1)$ and $A(\beta_2)$. Similarly, the second laboratory randomly chooses the displacement in the MZI setup to be $-\beta_3$ or $-\beta_4$, measuring observables $A(\beta_3)$ and $A(\beta_4)$. Both parties then perform a Bell-like experiment, similar to those in [13,16].

Each party possesses a pair of dichotomic observables with outcomes ± 1 ; hence, the celebrated CHSH inequality

$$|\mathbb{E}[A(\beta_1) \otimes A(\beta_3) + A(\beta_2) \otimes A(\beta_3) + A(\beta_1) \otimes A(\beta_4) - A(\beta_2) \otimes A(\beta_4)]| \leq 2 \tag{35}$$

should hold for classically correlated states. The expression on the left-hand side is a non-local observable. Its expected value is reconstructed from local measurements. If the absolute value of the expected value exceeds 2, the states of the two modes must be entangled.

The CHSH inequality can be violated if the maximal eigenvalue of the nonlocal observable it deals with exceeds 2. The maximum eigenvalue of the observable is equal to

$$\lambda_{\max} = 2\sqrt{1 + 4\sqrt{E_1(1-E_1)}\sqrt{E_2(1-E_2)}}, \tag{36}$$

where $E_1 = \exp(-|\beta_1 - \beta_2|^2)$ and $E_2 = \exp(-|\beta_3 - \beta_4|^2)$. The above expression attains its maximal value for $E_1 = E_2 = 1/2$, which corresponds to

$$|\beta_1 - \beta_2|^2 = |\beta_3 - \beta_4|^2 = \ln 2. \tag{37}$$

For such settings $\lambda_{\max} = 2\sqrt{2}$, which is exactly Tsirelson's bound for the standard CHSH inequality [17].

The entangled state for which the CHSH inequality is maximally violated is a projector onto the state vector:

$$\Psi = \frac{1}{2\sqrt{2 - \sqrt{2}}} \begin{pmatrix} -1 \\ 1 - \sqrt{2} \\ 0 \\ 1 - \sqrt{2} \\ 1 \\ 0 \\ 0 \\ 0 \\ 0 \end{pmatrix}. \tag{38}$$

The state lives in the two-qubit subspace of $\mathbb{C}^3 \otimes \mathbb{C}^3$. By calculating its partial trace, one can check that this is a maximally entangled state of two qubits. This is what we expect from a state maximizing the violation of the CHSH inequality.

Let us express the above state vector in terms of the state vectors $|\beta_i\rangle$. Using Eqs. (32), we obtain

$$\begin{aligned} |\Psi\rangle &= \frac{1}{2\sqrt{2 - \sqrt{2}}} \{[(1 - e^{i\phi_1} - \sqrt{2})|\beta_1\rangle + \sqrt{2}|\beta_2\rangle] \\ &\otimes [(1 - e^{i\phi_2} - \sqrt{2})|\beta_3\rangle + \sqrt{2}|\beta_4\rangle] \\ &- 2(2 - \sqrt{2})|\beta_1\rangle \otimes |\beta_3\rangle\}, \end{aligned} \tag{39}$$

where we have used the following:

$$\langle \beta_1 | \beta_2 \rangle = \sqrt{E_1} e^{-\beta_2 \beta_1^* + \beta_2^* \beta_1}, \quad (40)$$

$$\langle \beta_3 | \beta_4 \rangle = \sqrt{E_2} e^{-\beta_4 \beta_3^* + \beta_4^* \beta_3}, \quad (41)$$

substituting the maximizing values $E_1 = E_2 = \frac{1}{2}$ and introducing the notations $i\phi_1 = -\beta_2 \beta_1^* + \beta_2^* \beta_1$ and, similarly, $i\phi_2 = -\beta_4 \beta_3^* + \beta_4^* \beta_3$.

The above formula takes a particularly simple form if $\phi_1 = \phi_2 = 0$:

$$|\Psi\rangle = \frac{1}{\sqrt{2 - \sqrt{2}}} \{ [|\beta_1\rangle - |\beta_2\rangle] \otimes [|\beta_3\rangle - |\beta_4\rangle] - (2 - \sqrt{2}) |\beta_1\rangle \otimes |\beta_3\rangle \}. \quad (42)$$

For this condition to hold, we must have $\{\beta_1 \beta_2^*, \beta_3 \beta_4^*\} \in \mathbb{R}$; that is, the relative phases of β_1 and β_2 and β_3 and β_4 are zero.

B. CHSH inequality for finite intensities of coherent states

Until now we have assumed the ideal (limiting) case of $\alpha \rightarrow \infty$. Let us consider a more realistic scenario in which the intensity of the coherent state at the second input of the MZI is finite. In such a case, the dichotomic observable $A(\beta)$ (30) describing the photodetection changes such that $M_0(R', T\alpha)$, defined in (22), replaces the projector $|\beta\rangle\langle\beta|$. As generalized measurements are involved, the eigenvalue spectrum of the modified observables [say, $A_i(R', T\alpha)$] will be more complex than that of projective measurements. Thus, the reduction in the CHSH correlation matrix, i.e., the right-hand side of (35), to a finite-dimensional matrix (as performed in the preceding section) will no longer be possible. The maximal eigenvalue of such a CHSH correlation matrix with modified observables has to be calculated numerically, and we leave it for a future publication addressing this problem.

VI. CONCLUSION

We have devised a scheme for detecting entanglement in multiphotonic states using entanglement witnesses based on MZI setups. First, we showed that while a quantum beam splitter fed by a strong coherent laser beam can effectively displace an input quantum state, the MZI setup comprising 50:50 beam splitters and a small relative phase shift can actually implement this. For a many-photon input state, a generalized coherent state is observed at one of the output ports.

Next, we derived the uncertainty associated with the measurement observable (output intensity) when two different displacements are produced by the MZI setup. This uncertainty increases as a function of the difference between the displacements. Finally, we introduced entanglement witnesses that obey the CHSH inequality for testing entanglement in two-mode multiphotonic states. We also showed the structure of the entangled state that causes maximal violation of the CHSH inequality. It was found that such a state can be prepared using coherent states (which are, in fact, close to classical states).

However, note that certain restrictions are imposed on the bound of the CHSH inequality by the detector inefficiency. It was shown that if the detector efficiency falls down to $\gtrsim 85.4\%$, the bound in the CHSH inequality rises to Tsirelson's bound [26].

In the end, keep in mind that the MZI setup realizes the displacement operator in an approximate way; in fact, there is a trace amount of entanglement between output ports. As the second port is not measured, a POVM measurement is performed on the first port. The larger $|\alpha|$ is, the closer we get to a projective measurement.

ACKNOWLEDGMENTS

G.S. was supported by National Science Centre Project No. 2018/30/A/ST2/00837. M.G.D. was supported by the Prime Minister's Research Fellowship (PMRF), India.

APPENDIX A: DERIVATION OF POVM M_i

Considering the output state generated by the MZI setup with input $|\psi\rangle_0 \otimes |\alpha\rangle_1$ [analogous to Eq. (9) for the beam-splitter output state],

$$|\psi\rangle_0 \otimes |\alpha\rangle_1 \xrightarrow{\text{BS}} |\Psi\rangle_{\text{out}} = \hat{D}_4(R\alpha) \hat{D}_5(T\alpha) \sum_{n=0}^{\infty} c_n \frac{(T'\hat{a}_2^\dagger + R'\hat{a}_5^\dagger)^n}{\sqrt{n!}} |0\rangle_4 \otimes |0\rangle_5, \quad (A1)$$

where $c_n = \langle n | \psi \rangle$. The photon-annihilation operators corresponding to the output ports of the MZI setting are \hat{a}_4 and \hat{a}_5 (see Fig. 2). The projector on the state of this composite system is

$$\rho = \hat{D}_4(R\alpha) \hat{D}_5(T\alpha) \sum_{n=0}^{\infty} c_n \frac{(T'\hat{a}_4^\dagger + R'\hat{a}_5^\dagger)^n}{\sqrt{n!}} |0\rangle\langle 0|_4 \otimes |0\rangle\langle 0|_5 \sum_{n'=0}^{\infty} c_{n'}^* \frac{(T'^*\hat{a}_4 + R'^*\hat{a}_5)^{n'}}{\sqrt{n'!}} \hat{D}_4^\dagger(R\alpha) \hat{D}_5^\dagger(T\alpha). \quad (A2)$$

We can easily check that

$$\frac{(T'\hat{a}_4^\dagger + R'\hat{a}_5^\dagger)^n}{\sqrt{n!}} |0\rangle_4 \otimes |0\rangle_5 = \sum_{k=0}^n \sqrt{\binom{n}{k}} T'^k R'^{n-k} |k\rangle_4 \otimes |n-k\rangle_5. \quad (A3)$$

Therefore, Eq. (A2) reduces to

$$\rho = \sum_{n,n'} c_n c_{n'}^* \sum_{k=0}^n \sum_{k'=0}^{n'} \sqrt{\binom{n}{k} \binom{n'}{k'}} (T')^k (R')^{n-k} (T'^*)^{k'} (R'^*)^{n'-k'} \times \hat{D}_4(R\alpha) \hat{D}_5(T\alpha) |k\rangle \langle k'|_4 \otimes |n-k\rangle \langle n'-k'|_5 \hat{D}_4^\dagger(R\alpha) \hat{D}_5^\dagger(T\alpha). \quad (\text{A4})$$

The displaced photon-number state is observed at the output port corresponding to the annihilation operator \hat{a}_5 . Taking the partial trace over the first subsystem, we have

$$\rho_5 = \text{Tr}_4(\rho) = \sum_{n,n'} c_n c_{n'}^* \sum_{k=0}^{\min\{n,n'\}} \sqrt{\binom{n}{k} \binom{n'}{k}} |T'|^{2k} (R')^{n-k} (R'^*)^{n'-k} \hat{D}_5(T\alpha) |n-k\rangle \langle n-k|_5 \hat{D}_5^\dagger(T\alpha), \quad (\text{A5})$$

where we have used the cyclic property of the trace and $\hat{D}_4(R\alpha)^\dagger \hat{D}_4(R\alpha) = \mathbb{I}$. Now, detecting i photons from such a state can be represented by

$$\text{Tr}(|i\rangle \langle i| \rho_5) = \text{Tr} \left(e^{-|T\alpha|^2} \sum_{n,n'} \sum_{k=0}^{\min\{n,n'\}} \frac{|T'|^{2k} (R')^{n-k} (R'^*)^{n'-k} \sqrt{n!n'}}{k! \sqrt{(n-k)! (n'-k)!}} \sum_{j=0}^{\min\{i,n'-k\}} \frac{\sqrt{i!} (T'^* \alpha^*)^{i-j}}{\sqrt{j!} (i-j)!} \times \frac{\sqrt{(n'-k)!} (-T\alpha)^{n'-k-j}}{\sqrt{j!} (n'-k-j)!} \sum_{j'=0}^{\min\{i,n-k\}} \frac{\sqrt{i!} (T\alpha)^{i-j'}}{\sqrt{j'!} (i-j')!} \frac{\sqrt{(n-k)!} (-T^* \alpha^*)^{n-k-j'}}{\sqrt{j'!} (n-k-j')!} |n'\rangle \langle n| |\psi\rangle \langle \psi| \right) \quad (\text{A6})$$

using the cyclic property of the trace and calculating $\langle i | \hat{D}_5(T\alpha) | m \rangle = \langle -T\alpha | | m \rangle$, with $m \in \{(n-k), (n'-k)\}$, from Eq. (B6). We have also taken into account the fact that $c_n = \langle n | \psi \rangle$.

Therefore, the POVM element corresponding to measuring i photons at the detector end is

$$M_i = e^{-|T\alpha|^2} \frac{|T\alpha|^{2i}}{i!} \sum_{n,n'=0}^{\infty} (-R'^* T\alpha)^{n'} (-R^* T\alpha)^{*n} \sum_{k=0}^{\min\{n,n'\}} \frac{|R'\alpha|^{-2k}}{k!} \frac{\sqrt{n!n'}}{(n'-k)! (n-k)!} \times \sum_{j=0}^{\min\{i,n'-k\}} \frac{i! (n'-k)! (-|T\alpha|)^{-2j}}{j! (i-j)! (n'-k-j)!} \sum_{j'=0}^{\min\{i,n-k\}} \frac{i! (n-k)! (-|T\alpha|)^{-2j'}}{j'! (i-j')! (n-k-j')!} |n'\rangle \langle n|, \quad (\text{A7})$$

where we have used the Stokes law $R'T^* + R^*T' = 0$. Moreover, M_i takes into account moduli of R' , T , and T' . So their relative phases can be neglected. In the limits $T \rightarrow 0$, $|R'| = |R| \rightarrow 1$, and $\alpha \rightarrow \infty$, but $T\alpha$ remains constant; only the $k=0$ term dominates in the summation. So the form of M_i [from Eq. (A7)] in such a case is

$$M_i = \left(\frac{\exp(-\frac{|T\alpha|^2}{2})}{\sqrt{i!}} \sum_{n'=0}^{\infty} \sum_{j=0}^{\min\{i,n'\}} \frac{i! (T\alpha)^{n'-j} (-T^* \alpha^*)^{i-j}}{j! (i-j)! (n'-j)!} \sqrt{n'! |n'} \right) \text{H.c.} \quad (\text{A8})$$

On comparing the above with Eq. (B6) (up to relabeling of indices and changing the summation variable), we see that M_i reduces to a projector onto the generalized coherent state $|i, -T\alpha\rangle \langle i, -T\alpha|$.

APPENDIX B: GENERALIZED COHERENT STATES

The displacement operator acting on an n -photon state gives rise to generalized coherent states, given as

$$|n, \beta\rangle = \hat{D}(\beta) |n\rangle. \quad (\text{B1})$$

Now, applying the Baker-Campbell-Hausdorff formula to the displacement operator, we can expand the above expression as follows to obtain the exact functional form of $|n, \beta\rangle$:

$$|n, \beta\rangle = e^{-|\beta|^2/2} e^{\beta \hat{a}^\dagger} e^{-\beta^* \hat{a}} |n\rangle. \quad (\text{B2})$$

Using the Taylor expansion of exponents, we get

$$|n, \beta\rangle = e^{-|\beta|^2/2} \sum_{j=0}^{\infty} \sum_{i=0}^{\infty} \frac{(\beta \hat{a}^\dagger)^j (-\beta^* \hat{a})^i}{j! i!} |n\rangle. \quad (\text{B3})$$

The powers of creation and annihilation operators act on occupancy-number states as follows:

$$\hat{a}^{i,l} |m\rangle = \sqrt{\frac{(m+l)!}{m!}} |m+l\rangle, \quad \hat{a}^l |m\rangle = \sqrt{\frac{m!}{(m-l)!}} |m-l\rangle. \quad (\text{B4})$$

In Eq. (B3), we obtain

$$|n, \beta\rangle = e^{-|\beta|^2/2} \sum_{j=0}^{\infty} \sum_{i=0}^n \frac{(\beta)^j}{j!} \times \frac{(-\beta^*)^i}{i!} \sqrt{\frac{(n-i+j)!}{(n-i)!}} \sqrt{\frac{n!}{(n-i)!}} |n-i+j\rangle$$

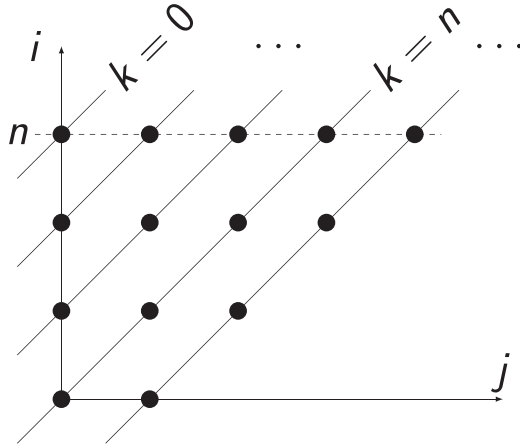


FIG. 6. Reparametrization of the summation area in (B5). The new variable k takes non-negative values. For a given k , the variable i takes values in the range $\{0, \dots, n\}$, except for $k < n$, for which the range of i is $\{n - k, \dots, n\}$.

$$\begin{aligned}
 &= \frac{e^{-|\beta|^2/2}}{\sqrt{n!}} \sum_{k=0}^{\infty} \sum_{i=\max\{0, n-k\}}^n \frac{(-\beta^*)^i}{i!} \\
 &\quad \times \frac{(\beta)^{k-n+i}}{(k-n+i)!} \frac{n!}{(n-i)!} \sqrt{k!} |k\rangle \\
 &= \sum_k C_{n,k} |k\rangle, \tag{B5}
 \end{aligned}$$

where the reparametrization has been done by introducing a new variable $k = n - i + j$ and the summation limits have been changed accordingly, as Fig. 6 explains.

One can easily check that expression (B5) can be reduced to a form involving associated Laguerre polynomials, as introduced in earlier papers [23,27]. However, if one needs to generate the whole matrix of the displacement operator, a slightly different representation of $C_{n,k}$ will be more convenient. After a reparametrization by $i \mapsto n - i$, one can express Eq. (B5) as follows:

$$\begin{aligned}
 C_{n,k} &= e^{-|\beta|^2/2} \sum_{i=0}^{\min\{n,k\}} \frac{(-\beta^*)^{n-i}}{(n-i)!} \frac{(\beta)^{k-i}}{(k-i)!} \frac{\sqrt{n!k!}}{i!} \\
 &= e^{-|\beta|^2/2} \sum_{i=0}^{\min\{n,k\}} \frac{\sqrt{n!}(-\beta^*)^{n-i}}{\sqrt{i!(n-i)!}} \frac{\sqrt{k!}(\beta)^{k-i}}{\sqrt{i!(k-i)!}} \\
 &= e^{-|\beta|^2/2} \langle u_n(\beta^*) | u_n(-\beta^*) \rangle, \tag{B6}
 \end{aligned}$$

where $|u_n(\beta)\rangle = \sum_{i=0}^n \frac{\sqrt{n!}(\beta)^{n-i}}{\sqrt{i!(n-i)!}} |i\rangle$. Hence, the matrix of the displacement operator in the occupancy eigenbasis can be decomposed as

$$D(\beta) = e^{-|\beta|^2/2} \mathbf{U}(\beta^*)^\dagger \mathbf{U}(-\beta^*), \tag{B7}$$

where columns of $\mathbf{U}(\beta)$ are the subsequent vectors $u_n(\beta)$. One can check that $\mathbf{U}(-\beta^*)$ is a matrix representation of $\exp(-\beta^* \hat{a})$. Hence, Eq. (B7) is a matrix representation of the operator equation (B2).

-
- [1] L. Caspani, C. Xiong, B. J. Eggleton, D. Bajoni, M. Liscidini, M. Galli, R. Morandotti, and D. J. Moss, *Light: Sci. Appl.* **6**, e17100 (2017).
- [2] F. Dell'Anno, S. De Siena, and F. Illuminati, *Phys. Rep.* **428**, 53 (2006).
- [3] W. Qin, C. Wang, Y. Cao, and G. L. Long, *Phys. Rev. A* **89**, 062314 (2014).
- [4] N. K. Langford, S. Ramelow, R. Prevedel, W. J. Munro, G. J. Milburn, and A. Zeilinger, *Nature (London)* **478**, 360 (2011).
- [5] P. Walther, K. J. Resch, T. Rudolph, E. Schenck, H. Weinfurter, V. Vedral, M. Aspelmeyer, and A. Zeilinger, *Nature (London)* **434**, 169 (2005).
- [6] V. Paulisch, M. Perarnau-Llobet, A. González-Tudela, and J. I. Cirac, *Phys. Rev. A* **99**, 043807 (2019).
- [7] I. Afek, O. Ambar, and Y. Silberberg, *Science* **328**, 879 (2010).
- [8] A. G. White, D. F. V. James, P. H. Eberhard, and P. G. Kwiat, *Phys. Rev. Lett.* **83**, 3103 (1999).
- [9] C. Schwemmer, G. Tóth, A. Niggebaum, T. Moroder, D. Gross, O. Gühne, and H. Weinfurter, *Phys. Rev. Lett.* **113**, 040503 (2014).
- [10] R. Horodecki, P. Horodecki, M. Horodecki, and K. Horodecki, *Rev. Mod. Phys.* **81**, 865 (2009).
- [11] M. Paris and J. Rehacek, *Quantum State Estimation*, Lecture Notes in Physics, Vol. 649 (Springer, Berlin, Heidelberg, 2004).
- [12] D. Chruściński and G. Sarbicki, *J. Phys. A* **47**, 483001 (2014).
- [13] J. S. Bell, *Phys. Phys. Fiz.* **1**, 195 (1964).
- [14] L. Maccone, *Am. J. Phys.* **81**, 854 (2013).
- [15] P. Hyllus, O. Gühne, D. Bruß, and M. Lewenstein, *Phys. Rev. A* **72**, 012321 (2005).
- [16] J. F. Clauser, M. A. Horne, A. Shimony, and R. A. Holt, *Phys. Rev. Lett.* **23**, 880 (1969).
- [17] B. S. Cirel'son, *Lett. Math. Phys.* **4**, 93 (1980).
- [18] A. Windhager, M. Suda, C. Pacher, M. Peev, and A. Poppe, *Opt. Commun.* **284**, 1907 (2011).
- [19] U. Leonhardt, *Rep. Prog. Phys.* **66**, 1207 (2003).
- [20] B. Yurke, S. L. McCall, and J. R. Klauder, *Phys. Rev. A* **33**, 4033 (1986).
- [21] H. Maassen and J. B. M. Uffink, *Phys. Rev. Lett.* **60**, 1103 (1988).
- [22] M. Boiteux and A. Levelut, *J. Phys. A* **6**, 589 (1973).
- [23] T. Philbin, *Am. J. Phys.* **82**, 742 (2014).
- [24] F. A. M. de Oliveira, M. S. Kim, P. L. Knight, and V. Bužek, *Phys. Rev. A* **41**, 2645 (1990).
- [25] R. Nehra, C.-H. Chang, Q. Yu, A. Beling, and O. Pfister, *Opt. Express* **28**, 3660 (2020).
- [26] J.-Å. Larsson, *Phys. Rev. A* **57**, 3304 (1998).
- [27] K. E. Cahill and R. J. Glauber, *Phys. Rev.* **177**, 1857 (1969).